Composites: Part A 67 (2014) 289–298

Contents lists available at ScienceDirect

Composites: Part A

journal homepage: www.elsevier.com/locate/compositesa

Characterization of the dynamic friction of woven fabrics: Experimental methods and benchmark results

U. Sachs [a], R. Akkerman [a,b,*], K. Fetfatsidis [c], E. Vidal-Sallé [d], J. Schumacher [e], G. Ziegmann [e], S. Allaoui [f], G. Hivet [f], B. Maron [g], K. Vanclooster [h], S.V. Lomov [i]

[a] TPRC Thermoplastic Composites Research Center, Palatijn 15, P.O. Box 770, 7500AT Enschede, The Netherlands
[b] University of Twente, P.O. Box 217, 7500AE Enschede, The Netherlands
[c] University of Massachusetts Lowell, Dept. of Mechanical Engineering, 1 University Ave, Lowell, MA 01854, USA
[d] Université de Lyon, INSA-Lyon, LaMCoS UMR5259 F-69621, France
[e] TU Clausthal, Institut für Polymerwerkstoffe und Kunststofftechnik, Agricolastr. 6, 38678 Clausthal, Germany
[f] Polytech'Orléans, Univ. Orléans, PRISME, EA 4229, F45072 Orléans, France
[g] TU Dresden, Institute of Lightweight Engineering and Polymer Technology (ILK), Holbeinstr. 6, 01307 Dresden, Germany
[h] Toray Industries Inc., Composite Materials Research Laboratories, 1515 Tsutsui Masaki-cho, Ehime 791-3193, Japan
[i] K.U. Leuven, Dept. of Metallurgy and Materials Engineering (MTM), Kasteelpark Arenberg 44, B-3001 Leuven, Belgium

ARTICLE INFO

Article history:
Received 10 March 2014
Received in revised form 19 August 2014
Accepted 24 August 2014
Available online 6 September 2014

Keywords:
A. Polymer–matrix composites (PMCs)
B. Friction
D. Mechanical testing
E. Forming

ABSTRACT

A benchmark exercise was conducted to compare various friction test set-ups with respect to the measured coefficients of friction. The friction was determined between Twintex®PP, a fabric of commingled yarns of glass and polypropylene filaments, and a metal surface. The same material was supplied to all benchmark participants and the test conditions were prescribed, making the used set-up the most important variable among the laboratories. Tests at ambient temperature as well as tests above the melting point of polypropylene are part of the benchmark, in order to determine both the dry and hydrodynamic friction characteristics. The dependency on sliding velocity, average pressure and temperature was investigated. Systematic differences are observed between the measurements obtained by the different set-ups, which are discussed and related to design characteristics of the devices. The values obtained in this benchmark are comparable and may serve as a reference to evaluate other friction set-ups. The paper concludes with guidelines for the design of a friction tester.

1. Introduction

Continuous fiber reinforced thermoplastic polymers provide advantageous properties, like a higher stiffness to weight ratio, compared to often used metals for structural applications. Comparing with their thermoset counterparts, they provide a better fracture toughness and infinite shelf live. Their ability to melt can also be exploited for automated forming and joining processes with relatively short cycle times, in the order of a few minutes.

An example of such a process is sheet forming of thermoplastic composites in a hot press. The process of forming a flat laminate to a 3D shape induces a number of different deformation mechanisms in the laminate. These can be classified by the length scale in which they occur [1,2]. The microscopic deformation mechanisms are the shear strain and elongation strain of each constituent (resin and fiber) and the contact mechanism between them. On a mesoscopic level the deformation may be perceived as fiber bending, resin percolation and transverse fiber flow. As the fiber redistribution and the change of the ply thickness is of less importance to describe the global deformation, we can turn to a macroscopic description of the deformation mechanisms in terms of ply bending, in-plane and inter-ply shear. These are the most common descriptions in literature, but other or additional definitions for the macroscopic mechanisms may be used, for example intra-ply extension or inter-ply rotation [1]. A delicate balance between the resistances to these deformation mechanisms determines the forming behavior of the laminate [3]. A precise characterization of these deformation mechanisms is necessary to accurately describe the composite forming process, to truly design for manufacturing in thermoplastic composites and to deploy their full potential. As a

* Corresponding author at: University of Twente, P.O. Box 217, 7500AE Enschede, The Netherlands.
E-mail address: r.akkerman@utwente.nl (R. Akkerman).

http://dx.doi.org/10.1016/j.compositesa.2014.08.026
1359-835X/

result, inter-ply shear or friction between the laminate and the tools is an often investigated mechanism and has led to numerous different testing devices and testing methods [4–9].

Literature that deals with inter-ply shear of composite sheets primarily focuses on wet friction, i.e. matrix in a molten state, while literature on dry friction of composite sheets, i.e. matrix in a solid state, is scarce. A short review of test methods of wet friction with controversial issues is presented next.

Groves began investigating inter-ply shear using a Rheometrics Dynamic Spectrometer [4]. A stack of several plies was placed between two parallel disk platens and subsequently subjected to an oscillatory torsional deformation (Fig. 1a), maintaining a constant temperature above the melting point of the polymeric resin. The resistance against shear can be calculated in terms of a dynamic viscosity from the measured torque and the rotation angle. Groves was able to relate the dynamic viscosity to the steady shear viscosity by describing the fluid behavior with a Maxwell model. His experiments also indicated that the shear deformation was not only restricted to inter-ply resin rich layers, but was also accompanied with intra-ply shear. Typically, for this type of composites the transverse shear stress increases with the shear velocity. Influences of the temperature or normal pressure were not considered, yet.

Scherer and Friedrich [5] determined the inter- and intra-ply shear by drawing a single ply out of a stack of plies (Fig. 1b), maintaining a constant slip velocity. A hot platen press was used to keep the temperature constant and above melt temperature throughout the slip process. Only slight pressure was applied to ensure contact of the heating platens with the specimen. Also here the shear stress increased with higher slip velocity. While Groves could not find large differences between cross-ply and parallel ply configurations, the experiments of Scherer et al. did show a large influence of the lay-up of the composite. These experiments captured also the transient starting effects, showing a gradual increase of the shear stresses, until a steady state situation was reached.

Morris and Sun [6] prepared specimens consisting of two outer sublaminates and a central sublaminate. The specimen was clamped between two heated platens, by means of a clamp. The applied pressure was determined by strain gauges attached to the clamp and only acted on the overlap of the sublaminates (Fig. 1c). The central sublaminate was pulled out during the test. These experiments led to an initial peak force which exceeds the later steady state value, which was not observed in [5]. Both peak and steady state stresses showed an exponential increase for increasing sliding velocities, while they were considerably decreasing when increasing the temperature from below the melt temperature to

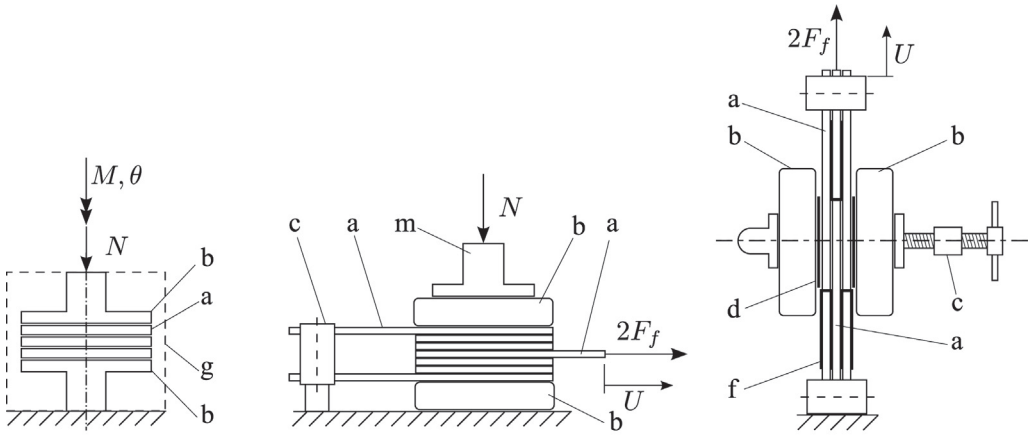

(a) Groves [4], material: UD carbon PEEK and UD glass PEEK.

(b) Scherer *et al.* [5], material: UD carbon PP.

(c) Morris and Sun [6], material: UD AS4/PEEK.

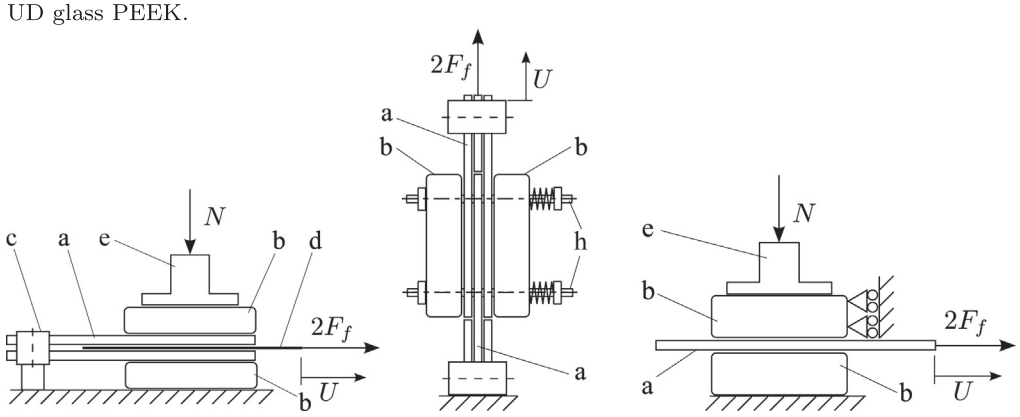

(d) Murtagh *et al.* [7], material: UD AS4/PEEK

(e) Lebrun [8], material: 2/2 twill glass/PP (Twintex)

(f) Gorczyca-Cole *et al.* [9], material: 2/2 twill glass/PP (Twintex)

Legend:

a: composite specimen	b: plate/ heated plate	c: clamp	d: steel foil
e: press	f: release film	g: climate chamber	h: axis of springs

Fig. 1. Friction test set-ups in the literature.

above the melt temperature. Against their expectations, increasing the normal pressure led to higher shear stresses. Morris and Sun suspected that the higher shear stress was caused by a decrease of the film thickness and frictional contact between adjacent plies.

The measurement set-up designed by Murtagh et al. [7] is similar to that of Scherer et al. but the intra-ply shear is prevented by fixating the fibers of each ply, enforcing inter-ply slip between laminate and tooling, i.e. tool–ply slip (Fig. 1d). Rather than using the shear stress, the results were expressed in terms of the apparent coefficient of friction (CoF), as it is the traditional method of presenting friction results [10]. The determination of the CoF is based on ASTM standard D1894 [11], which assumes a simple Amontons-Coulomb friction behavior. Murtagh et al. investigated the same material as Morris and Sun (AS4-PEEK), observing also an initial peak of the CoF and the same trends in velocity and pressure dependency. Increasing the temperature, however, led to an increase of the CoF, in contrast to the earlier reported results. This effect was ascribed to a thickness reduction of the resin rich inter-layer.

The experimental set-up used by Lebrun et al. [8] is similar to the one of Morris and Sun, investigating inter-ply shear as well as tool/ply shear (Fig. 1e). The obtained results are largely in agreement with the previous studies. An increase in temperature, however, was found to slightly decrease the CoF in the case of inter-ply shear, and to increase the CoF in the case of tool/ply shear. This contradicting observation was interpreted as an effect of Coulomb friction caused by tool–fiber interaction.

In contrast to the previous set-ups Gorczyca-Cole et al. [9] applied a pull-through test, meaning that the test specimen sticks out at both ends of the test area, such that the sheared area does not decrease during the test and the applied pressure remains constant (Fig. 1f). Furthermore, a uniform pressure distribution can be maintained. It was found that the friction behavior can be described by the Stribeck theory, which relates the CoF exclusively to the Hersey number, defined as:

$$H = \frac{U\eta}{p}, \tag{1}$$

where U, η, and p, denote the shear velocity, matrix viscosity and normal pressure, respectively.

These examples show that various custom-built set-ups were developed to determine the inter-ply and tool/ply shear behavior, all differing in design and sizes. Since no general standard exists for testing thermoplastic composites at process conditions, each research group developed their own procedure, resulting in different results for similar materials. A benchmark exercise has been launched on the 13th Esaform conference (2010), to clarify whether design differences have a significant effect on the measurement results.

2. Benchmark description

Different friction measurement devices were benchmarked by comparing the measured dynamic CoF values. The benchmark prescribes the material and the conditions to be applied, ensuring the comparability of all results. Still, the preparation of the samples and the detailed test procedure may vary for different devices, due to their characteristic properties and capabilities, e.g. size or heating power.

2.1. Material

The friction coefficient between Twintex®PP and mild steel has been measured in this benchmark. The choice for Twintex®PP is taken, since it is readily available, and it was subject of earlier investigations [8,9,12]. Moreover, its relatively low melting temperature is less demanding for the design of the friction test set-up. Twintex®PP is a fabric consisting of commingled glass and polypropylene (PP) yarns. Dry fabrics and pre-consolidated plates were kindly supplied by Vetrotex. Further material properties of the composite are given in Table 1. The linear count of filaments in warp and weft direction is equal, while the warp count and the weft count, which measures the number of fiber bundles per length and width respectively, are unequal. Fig. 2a shows the geometrical unbalance, exhibiting a larger undulation of the smaller warp bundles than of the weft bundles.

A commercially available mild steel foil M-Tech®F was used, to ensure equal metal surface properties for all test participants. Its material properties are given in Table 2. Before testing, the foil was cleaned from residual grease with an adequate solvent, e.g. acetone.

Tests at ambient temperature were conducted with unconsolidated fabric, while pre-consolidated plates were used for tests above the melting temperature. All participating research groups were provided with unconsolidated and pre-consolidated Twintex from the same batch as well as steel foil.

The viscosity (η) of neat polypropylene is required for the analysis of the experimental results. Polypropylene granulate of the same grade as the Twintex®PP matrix material was investigated by Vanclooster [12]. He determined the limits of process temperatures, reaching from the melting temperature of 165–230 °C, where the polypropylene starts to degrade. He also performed dynamic oscillatory shear experiments to characterize the bulk viscosity. The sinusoidal oscillation and material responses are written in complex form, resulting in a complex viscosity notation. The norm of the complex viscosity is plotted against the angular frequency in Fig. 3 for different temperatures. The graphs show plateau values η_0 at low shear rates. These values are used to characterize the temperature dependent material viscosity, used in further analyses.

2.2. Test matrix

The test conditions are defined by temperature T, sliding velocity U, and average pressure $p = N/A$, where N denotes the normal force on the friction area A. The test matrix is given in Table 3 showing a set of test parameters which form the baseline conditions. Additional to the baseline conditions either the temperature, pressure or sliding velocity was varied. The additional values are also summarized in Table 3. The sliding direction was always parallel to the warp-direction (Fig. 2a). Pulling in weft-direction has a higher risk of tearing the fabric apart [13], which can be explained by the low undulation of the weft yarns (Fig. 2b), allowing the warp-yarns to slide easily along the weft-direction. Experiments were performed in triplicate for each single condition.

2.3. Criteria

Only the dynamic coefficient of friction was determined for friction at ambient temperature, since the static coefficient of friction,

Table 1
Properties of Twintex®T PP 60 1485.

Property	Value
Weight % glass	60%
Areal weight	1485 g/m^2
Plate thickness	Approx. 1 mm
Weave type	Balanced 2 × 2 twill
Warp count	377 m^{-1}
Weft count	168 m^{-1}

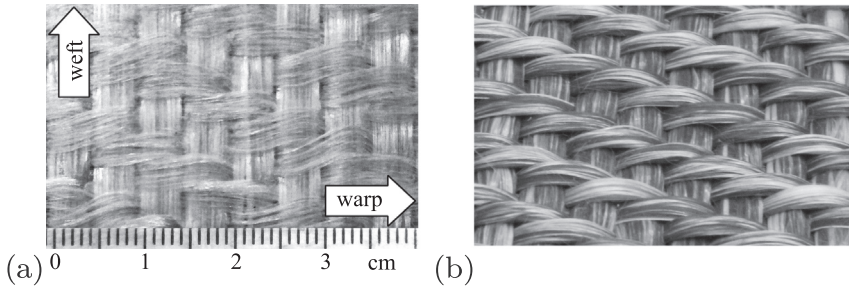

Fig. 2. 2 × 2 Twintex® glass polypropylene: (a) preconsolidated plate and (b) unconsolidated fabric.

Table 2
Properties of the applied mild steel foil.

Property	Value
Material	Mild steel
Thickness	0.05 mm
Tolerance	±0.005 mm
Standard	EN 10139
Roughness	R_a = 0.2 μm

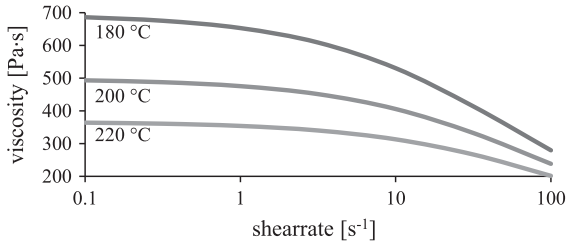

Fig. 3. Viscosity measurement of neat polypropylene measured by Vanclooster [12].

Table 3
Test matrix for ambient temperature and above melting temperature.

Parameter	Dry friction		Wet friction	
	Baseline value	Additional values	Baseline value	Additional values
Temperature (°C)	23		180	200, 220
Pressure (kPa)	20	10, 40, 100	20	10, 40, 100
Velocity (mm/min)	60	20, 200, 1000	60	20, 200, 1000

which may differ only slightly from the dynamic coefficient, could not be measured by every research group. This is described in more detail in Section 4. Both types of friction were investigated for experiments conducted above the melt temperature.

3. Measurement devices of participants

All participants have developed their own set-up, which measures the friction force F_f between the test materials, while keeping the normal force N, sliding velocity U and temperature T constant. Differences between the set-ups are the size of the friction area A, ranging from 300 to 10,000 mm^2 (summarized in Table 4), and the mechanism that distributes the normal force over the friction area. Details about the mechanims of each set-up are presented in the following subsections.

3.1. University of Twente

The measurement device developed at the *University of Twente* [14] (Fig. 4a) operates in a universal testing machine. A flexible pneumatic actuator supplies the normal load N in a self-aligning system. The normal load is measured by three load cells, which also allow to record resulting moments exerted around the center of gravity of the contact surface. Thick blocks minimize the tool deflection, whereas the overlapping edges are used to pre-heat the laminate before it enters the friction area, A, of 2500 mm^2. Temperatures are measured in both blocks with multiple thermocouples. The homogeneity of the pressure and the temperature field was investigated and optimized [15,16].

3.2. University of Massachusetts Lowell

The *University of Massachusetts Lowell* (*UML*) has designed a set-up (Fig. 4b), that encloses the entire test specimen between the pressure plates throughout the experiment. This leads to a constant average pressure, since the size of the friction area remains constant, which is 4000 mm^2. However, the normal force is not acting on the center of the test area, which leads to a non-uniform pressure distribution.

The normal force, exerted by an air-spring system, is feedback controlled by compression load cells. The measurement device was designed to apply sliding velocities U up to 5000 mm/min and pressures p of more than 1.8 MPa. The benchmark conditions are at the lower end of this devices processing window, resulting in noise in the measured data. The noise was reduced by post-processing the data.

3.3. TU Clausthal

The experimental set-up at the *Clausthal University of Technology* (Fig. 4c) consists of two parallel vertical steel plates of 10,000 mm^2, which can be displaced laterally along the sides of a horizontal base plate. Composite laminates are mounted on both steel plates, by means of double faced adhesive tape. A moving part intended to be pulled out during the experiment (in this case the steel foil) is positioned and clamped between the parallel plates. The cumulative clamping force N is applied by means of four linear elastic compression springs. The compression of each spring can be regulated by tightening or loosening the adjusting nuts. The set-up is mounted in a universal testing machine equipped with a 10 kN load cell to measure the pulling force F_f. The crosshead of the universal testing machine is position controlled and moves with a constant velocity U.

3.4. Université d'Orléans

The principle of the apparatus used at the University of Orléans [17] is shown in Fig. 4d. It has been designed to characterize the frictional behavior of fabric/fabric, fabric/steel and yarn/yarn friction. It is based on two plane surfaces sliding relative to each other, making contact over an area of 1600 mm^2. The bottom specimen is fixed on a rigidly and accurately guided steel plate. The required

Table 4
Dimensions of the nominal friction area A per group.

	TU Clausthal	KU Leuven	UML	TU Dresden	University of Twente	University of Orléans	INSA Lyon
$L \times W$ (mm × mm)	100 × 100	80 × 80		150 × 20	50 × 50	40 × 40	15 × 20
Area (mm^2)	10,000	6400	4000	3000	2500	1600	300

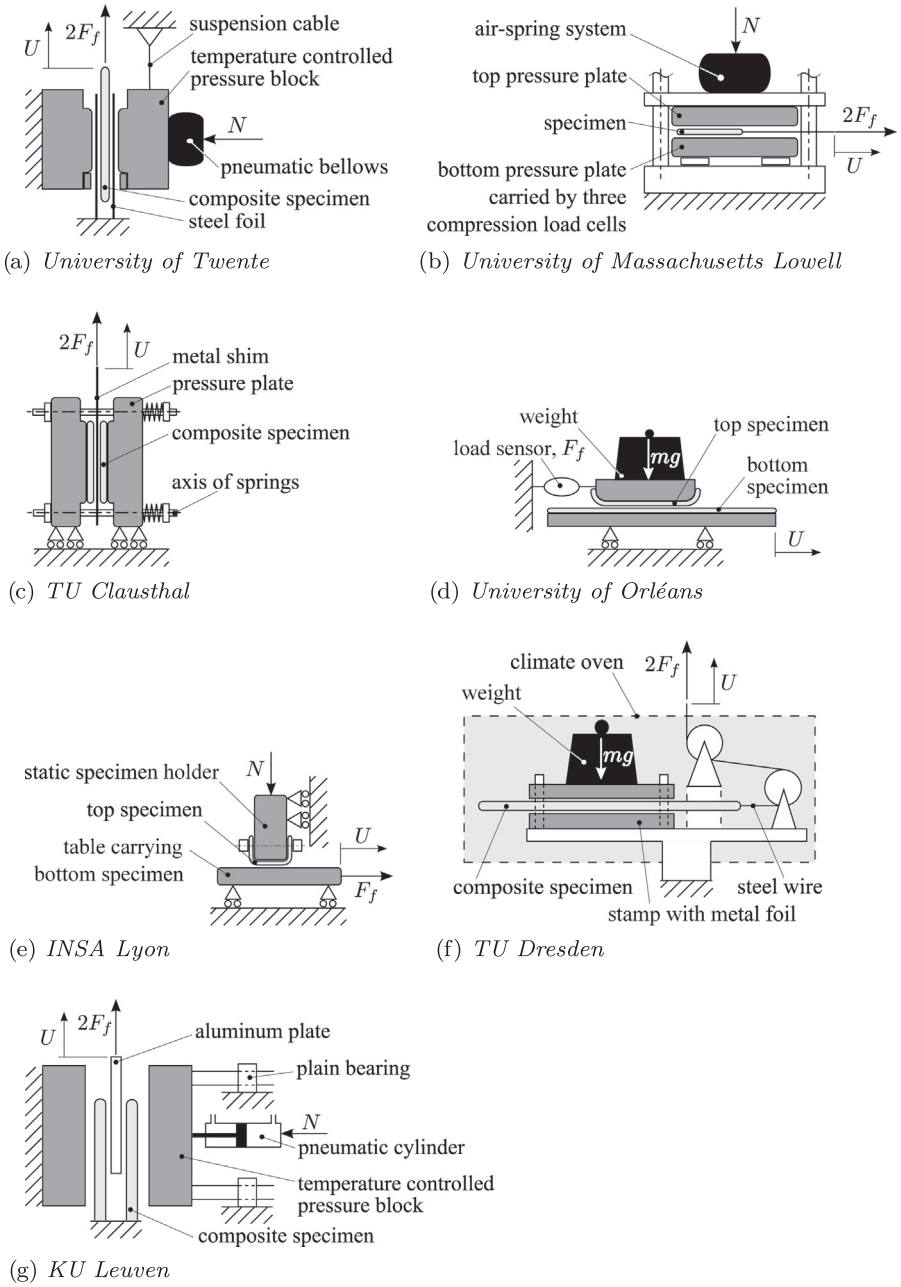

Fig. 4. Schematic representation of the friction test set-ups of the benchmark participants.

velocity is imposed by an electronic controlled motor. The top specimen is fixed on a steel plate which is linked to the load sensor. A rubber damper is chosen to limit the vibrations and enable a smoother signal. A dead weight provides the constant normal load N. A calibration procedure determines the optimal position of the dead weight to obtain a uniform pressure distribution on the contact area. The angle between the samples can be adjusted by rotating the upper sample. In addition, the contact surfaces can be reduced in order to achieve higher pressure contact.

3.5. INSA Lyon

The testing device designed at *INSA Lyon* is presented in Fig. 4e. The top specimen is mounted under a static specimen holder,

having a size of 300 mm^2. A table carrying the bottom specimen is displaced laterally by a pneumatic actuator. A linear variable differential tranformer (LVDT) measures the displacement of the table, while a load cell measures the load exerted by the actuator. Another load sensor measures the normal load. In order to obtain the net friction force F_f, the resistance of the table guidance needs to be subtracted from the actuator load. The guidance resistance is determined prior to the friction experiment, by applying only weights on the table, which are equivalent to the normal load. The angle between the two specimens (i.e. sliding orientation) can be adjusted by rotating the static specimen holder. Since the sliding velocity is governed by the air pressure we can speak of a force controlled system.

3.6. TU Dresden

A textile friction measurement device was developed at the *University of Dresden*, which is applicable for universal testing machines. The maximum possible sliding velocity is 1000 mm/min. The specimen is pulled through an upper and a lower stamp of 3000 mm^2, on which a metal foil is fixed (Fig. 4f). It is possible to regulate the normal pressure with a dead weight or with a pneumatic cylinder for higher pressures. A dead weight was used for the benchmark experiments reported here. The temperature is controlled by placing the entire set-up into the oven of the universal testing machine. The devices resistance induced by the pulleys and steel wire bending was determined, and a correction on the pulling force was applied.

3.7. KU Leuven

Fig. 4g presents the set-up of the pull-out machine used at the *University of Leuven*. It consists of two temperature controlled steel plates, which are mounted in a frame, installed in a universal testing machine. The normal force on the specimens is applied by a hydraulic cylinder. The homogeneity and the magnitude of the pressure and the temperature field were verified for the starting position of the test configuration [12]. In contrast to the other set-ups, the friction area of initially 6400 mm^2 does not remain constant, but decreases while the specimen is pulled out, leading to an increasing average pressure as the test proceeds. Simultaneaously, a non-uniform pressure distribution is to be expected, when the static normal force is no longer acting in the center of the upwards moving test area.

4. Results for dry friction

4.1. Results

Five benchmark participants have conducted dry friction measurements. An example of friction measurements obtained by *TU Clausthal*, *University of Twente*, *University of Orléans* and *UML* is shown in Fig. 5. A steady state CoF is reached after a short start transition. *University of Twente* and *UML* measured a gradual increase at the start, which may be explained by the stretching of the Twintex fabric, that is pulled. *University of Orléans* and *TU Clausthal* mounted the fabric to the pressure plates instead, which is a good measure to reduce the stretch of the fabric. These set-ups were able to measure a minor friction peak, that is considered as the initial static friction. In this paper we focus on the dynamic friction. The summarized results are presented in Fig. 6. The CoF values measured by the participants differ from 7% to 32%. The smallest difference is observed with 60 mm/min sliding velocity and 20 kPa pressure, while the highest difference occurs at 1000 mm/min and 20 kPa. Most research groups achieved small

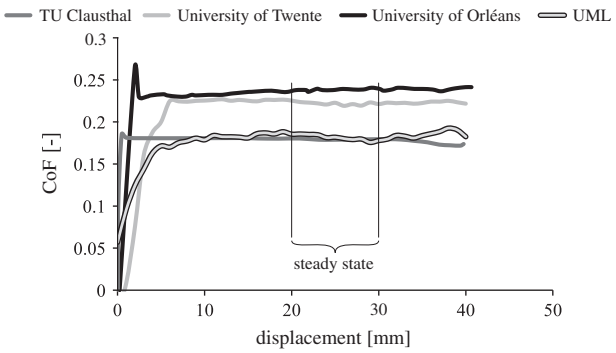

Fig. 5. Exemplary friction measurement conducted at $T = 23$ °C; $p = 20$ kPa and $U \geqslant 200$ mm/min. *TU Clausthal* and *University of Orléans* observed a minor friction peak. The steady state friction is defined arbitrarily between 20 and 30 mm displacement.

standard deviations with an average coefficient of variation of less than 5 %. *University of Twente*, *University of Orléans* and *TU Clausthal* measured a slight decrease of the CoF when increasing the pressure at low sliding velocities (Fig. 6b). This trend, however, is not observed anymore at high sliding velocities (Fig. 6c).

4.2. Discussion

The low coefficient of variation indicates a high measurement precision, which signifies a good reproducibility of repeated CoF measurements, as it is commonly defined [18]. But it does not necessarily indicate a high measurement accuracy in measuring the true CoF. Moreover, a systematic error may be present, which becomes clear by the systematic differences between the research groups. Values of *TU Clausthal* are constantly lower than those of the *University of Orléans*, while most values of *UTwente* lie in-between.

Despite an uncertain offset, it can be concluded that the friction behavior is fairly well described with the Amontons-Coulomb model, which states that the CoF is independent of the sliding velocity and normal force. The measured values at 20 kPa pressure and sliding velocities between 20 and 1000 mm/min (Fig. 6), remain between 0.26 and 0.18 without exhibiting a clear trend.

The CoFs at the highest sliding velocity of 2400 mm/min measured by *INSA Lyon*, are relatively low and exhibit large standard deviations. The comparatively small nominal friction area (see Table 4) leads to friction-forces of small magnitude, which might lead to precision problems, if spurious (e.g. edge) effects do not scale down with the friction area in the same degree.

In general, attention has to be paid to the structural rigidity of the friction set-up. As it was shown by ten Thije and Akkerman [15] a deflection of the pressure plates may have substantial influence on the pressure distribution. Likewise, misalignments of the friction surface caused by the friction force have to be considered. Fig. 7a shows a concept of a test set-up with a high offset from the pressure plate support to the friction surface. The degree of rotation of the plate depends on the structural stiffness in lateral direction, and will result in a pressure gradient over the friction area. The misalignment can either be avoided by a high structural stiffness, or by diminishing the rotating moment itself. The latter can be achieved by supporting the pressure plate close to the friction surface as shown in Fig. 7b, and is realized by *University of Twente* and *KU Leuven* by clamping the outer specimens directly to the support structure and not to the pressure plate (Fig. 4a and g). Another solution to reduce the rotating moment is to adapt the position of the normal force N, as shown in Fig. 7c. *University of Orléans* has accomplished this by an optimal positioning of the dead weight, to regulate the center of gravity of the structure

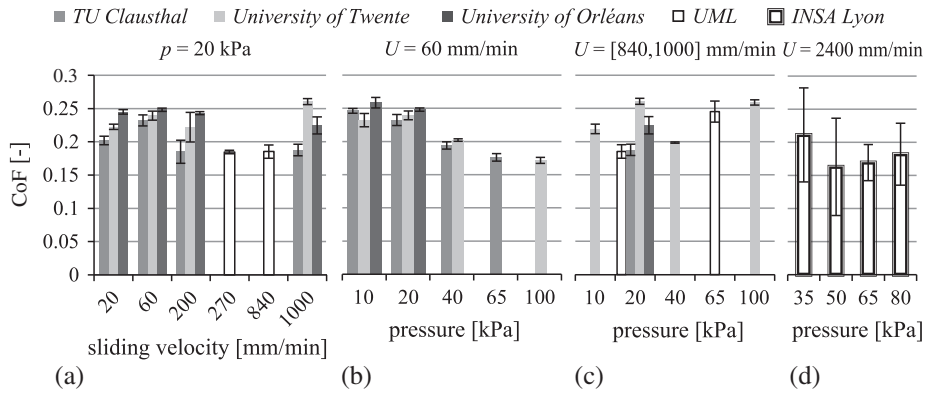

Fig. 6. Steady state friction coefficients for dry friction experiments, (a) at $p = 20$ kPa and varying velocity, (b) at $U = 60$ mm/min and varying average pressure, (c) at $U = 840$ mm/min (*UML*) and $U = 1000$ mm/min (*TU Clausthal*, *University of Twente* and *University of Orléans*), and (d) at $U = 2400$ mm/min (*INSA Lyon*).

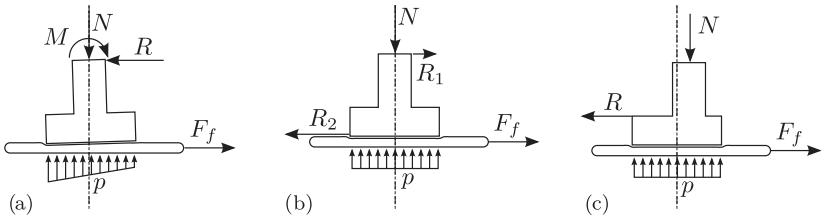

Fig. 7. (a) Misalignment due to friction force and compliant supporting structure; diminishing the rotating moment on the pressure plate by (b) a low offset from reaction force and friction surface or (c) a repositioning of the normal force.

(i.e. dead weight, specimen holder and top specimen) (Fig. 4d). Its positioning depends on the magnitude of the friction and the normal force and requires a calibration procedure. The set-up of *INSA Lyon*, on the other hand, is relying on a stiff guidance of the static specimen holder, since the support has comparatively high offset to the friction surface (Fig. 4e).

Excluding *INSA Lyon*, the friction coefficients appear to be larger when the friction surface is smaller. This might be caused by spurious edge effects which scale with the length of the block edges and not with the friction surface. In case of a pull-through experiment, new material that is pulled into the contact area, needs to be compressed or is subjected to additional shear. *UML* and *TU Clausthal* have minimized this effect by letting the metal surface entering the contact area, which is smooth and incompressible compared to the Twintex fabric. *University of Twente* applies chamfered edges and the steel foil to guide the fabric into the contact area. Also *University of Orléans* and *INSA Lyon* have designed their top specimen holder with rounded edges, to reduce edge effects.

All friction testers in the benchmark have in common, that the normal force is applied on a fixed position. Therefore, a static sliding contact area allows for a better maintenance of a uniform pressure. *UML* has a moving contact area, and a changing gradient in the pressure distribution is conceivable. Nevertheless, the experimental results for the Twintex fabric do not seem to be affected during the tests at *UML* (Fig. 5).

5. Results for wet friction

5.1. Results

In contrast to the dry friction experiments of Twintex fabric, the wet friction results show a hydrodynamic friction behavior, similar to the findings of other researchers [8,9,19], who examined the same material. A typical example of these friction experiments is shown in Fig. 8, showing an initial friction peak and a tendency towards a steady state at the end of the experiment. Both states of friction, denoted as the peak CoF and the steady state CoF respectively, are investigated in this benchmark. Fig. 9 summarizes the peak and the steady state values of the CoF at the tested conditions. The steady state is defined between 20 and 40 mm displacement for measurements performed by *UTwente* and *KU Leuven*. The *KU Leuven* results were obtained for variable conditions during the experiment and required extra post processing, as will be discussed in the next section. For *TU Dresden* a steady state is reached between 55 and 70 mm displacement. Both the peak and the steady state CoF exhibit typical hydrodynamic trends, as their values increase with increasing velocity and decreasing pressure. In general, an increasing temperature leads to decreasing CoF values.

Additionally, an analytical model can be applied [19] to predict the steady state friction. The model is based on shear flow calculations of the thermoplastic matrix. The flow is confined by an idealized geometry that represents the fiber bundles of the reinforcement and the flat metal surface. Model and experimental results show the same trends (Fig. 9a).

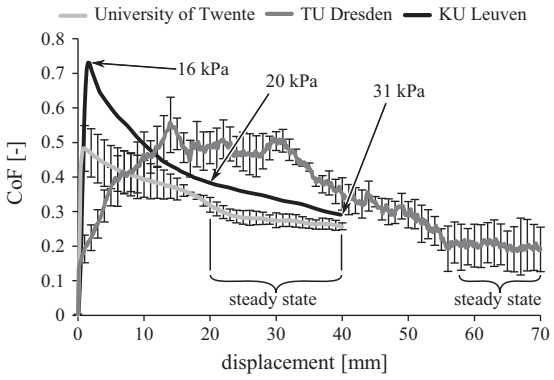

Fig. 8. Exemplary friction measurement conducted at $T = 180$ °C; $p = 20$ kPa and $U = 60$ mm/min measured by three different benchmark participants, *KU Leuven* has varying pressure conditions.

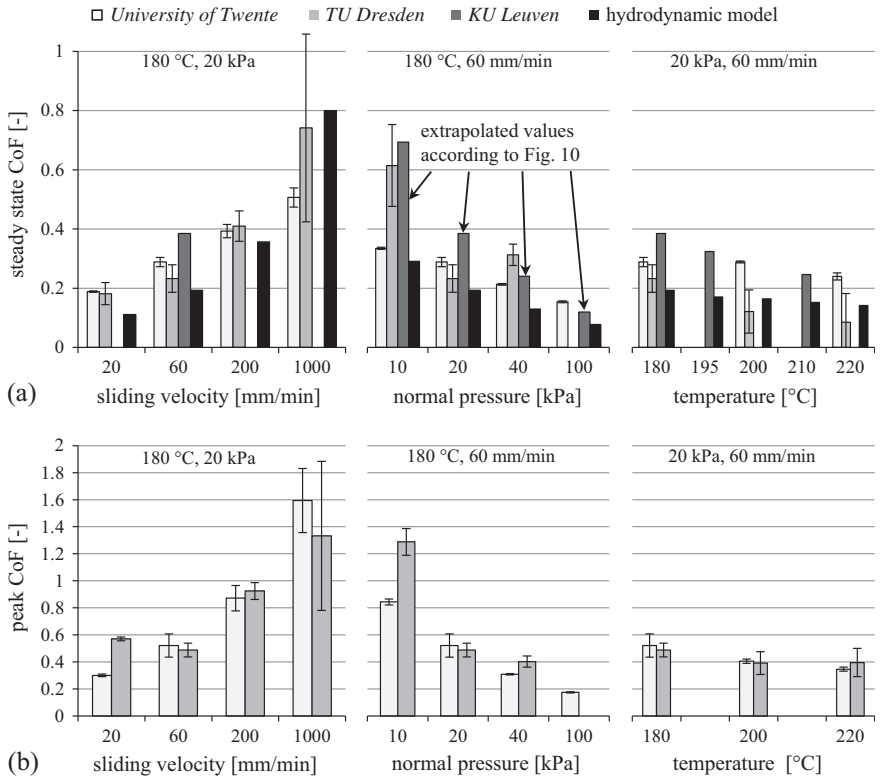

Fig. 9. (a) Steady state and (b) peak coefficients of friction for the wet friction experiments. The *KU Leuven* steady state results were determined from Fig. 10.

5.2. Discussion

The temperature dependency of the friction is different from Lebrun's findings [8]. While the benchmark participants have found a decreasing effect on the friction, Lebrun's experiments showed an increasing effect. What looks contradictory at the first glance, might be explicable by slightly different test conditions. Lebrun applies a higher average pressure and a lower pull velocity (p = 70 kPa and U = 20 mm/min). For these conditions and a matrix viscosity at a temperature of 200 °C, the analytical model predicts a remaining thermoplastic film thickness between the glass fabric and the metal surface of 25 µm. This approaches the filament diameter of the glass fibers, which is seen by ten Thije et al. [19] as the transition point between pure hydrodynamic lubrication and mixed lubrication. Also Lebrun assumed contact between metal and fiber as a reason for his unexpected results.

The peak friction shows the same trends caused by velocity, pressure and temperature variation as the steady state friction. Murtagh, who observed the initial peak friction for APC-2 composites, was interpreting this phenomenon as an adhesive bond that has to be overcome. He suggested that the creation of the bond is caused by the intimate contact between the composite and the metal surface while the set-up is heated up [7]. Morris and Sun, who also refer to it as a yield stress, showed that the initial yield strength can be recovered after ceasing the motion for only 10 s [6]. Therefore, the initial peak should be largely independent of the heat-up duration, provided that no polymer degradation takes place. Another cause of the transient maximum stress might be the rheological behavior of a visco-elastic fluid. The same kind of shear stress growth, that is observed in the friction experiments, is exhibited by many polymeric fluids upon the inception of a steady shear flow [20]. Additionally, the subsequent stress decrease to a steady state value might be supported by a gradual development of the lubricating layer.

Comparing the friction data obtained by the different benchmark participants, a certain agreement of peak and steady state friction values between *University of Twente* and *TU Dresden* can be seen in Fig. 9b from their intersecting confidence intervals (twice the standard deviation). This might be surprising when considering the example measurement of the two institutes shown in Fig. 8. The measurement curve obtained by *TU Dresden* reaches the peak and steady state values at a much later state and exhibits more noise. This indicates stretching of the specimen, which is heated entirely in a heating chamber. Since force and displacement sensors need to be protected from the heat, they are placed in safe distance to the specimen, adding an extra compliance of the transmission to the measurement.

A small inconsistency in the measurements of the *TU Dresden* may be suspected, since the data point at the test condition of 20 kPa, 60 mm/min and 180 °C, forms a local minimum in one of the trend curves of the steady state and the peak CoF. This inconsistency does not go along with a noticeable high standard deviation and may therefore be attributed to a systematic error appearing for low sliding velocities. For such complex set-ups it is very difficult to isolate the origin of this error, and a very strict testing procedure may help at least for obtaining consistent results.

The measurements obtained by *KU Leuven* cannot be compared directly with the other measurements, because most tests are performed at 195 °C instead of 180 °C while adopting a pull-out instead of a pull-through test configuration (compare Fig. 4a, f and g). This implies a gradual decrease of the friction area from initially 80 × 80 mm^2 to 40 × 80 mm^2 after 40 mm displacement. The applied normal force remains constant during the test, resulting in a progressive increase of the average pressure. Strictly speaking, a steady state condition is not reached as it can be seen in Fig. 8. The measurement curve obtained by *KU Leuven* while applying a constant normal force of around 100 N remains declining after

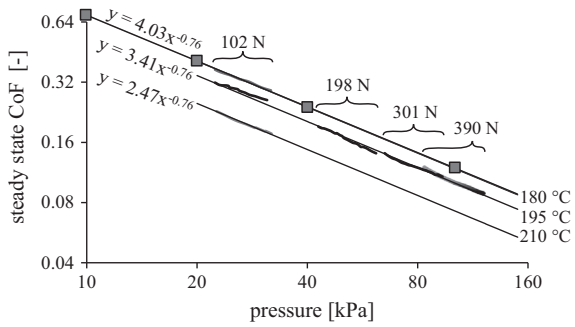

Fig. 10. *KU Leuven*. Experimental results (bold line segments) for the steady state CoF versus the average pressure, measured at $T = 180\,^{\circ}C$, 195 °C, 210 °C and $U = 60$ mm/min, between 20 and 40 mm displacement. The fitted curve (Eq. (2)) for 180 °C was used to determine the CoF values for $p = 10$, 20, 40 and 100 kPa (the square symbols), as presented in Fig. 9.

20 mm displacement, due to the pressure increase. Assuming that the rate of pressure change is sufficiently low, a "quasi-steady state" may be reached. Consequently, the "steady state" CoF (between 20 and 40 mm displacement) can be plotted as a function of the current average pressure on a double logarithmic scale, represented by the thick line segments in Fig. 10. Indeed, it appears that the curves for different normal forces, obtained at 195 °C and 60 mm/min sliding velocity, are well in line, meaning that the steady state CoF is fairly independent on the displacement. The line segments were curve fitted with a power law,

$$\mu = C(T) \cdot \bar{p}^{n}, \tag{2}$$

with μ as the CoF and $\bar{p}$ as the average pressure, showing good correlation with the experimental results. The fitted curve for 180 °C, was used to estimate the *KU Leuven* values, presented in Fig. 9 a for $U = 60$ mm/min. It should be noted that we are only comparing conditions between 20 and 40 mm displacement. Influences by the displacement on the CoF may still be significant during the first 20 mm of displacement, and different for the various test set-ups. The curves in Fig. 10 can be described closely by a power law. Considering, that the lines for different temperatures should not intersect, the exponents have to be equal. Based on these considerations, it was possible to extrapolate the steady state CoF for 180 °C to different pressures as it is done to obtain Fig. 9a.

The steady state values of *KU Leuven* represented in Fig. 9 are in general higher than those of *UTwente* and show a stronger dependency on pressure and temperature. The high standard deviation of the *TU Dresden* results make it hard to distinguish the trends. A definite conclusion cannot be drawn from the limited number of data points that are compared with each other in these graphs.

For the ease of comparability, a representation of all data points in a master curve is beneficial. The so-called Stribeck curve can be used for this purpose [9]. It relates the CoF to a single parameter, known as the Hersey number. Its definition (1) requires the quantification of the matrix viscosity η of the neat thermoplastic resin. Its value is approximated by the zero shear viscosity η_0 (given in Fig. 3), since the actual viscosity depends on the unknown shear rates within the resin. In this way the effect of the temperature T on the coefficient of friction is accounted for. The Stribeck plot of all high temperature friction test results is presented in Fig. 11.

A Stribeck curve representation is very accurate for the applied hydrodynamic lubrication model as indicated by the high R-value of the exponential fit in Fig. 11a. Besides the steady state friction predicted by the model, the measured data from *UTwente* and *KU Leuven* are also closely approximated by an exponential function. The data from *TU Dresden* on the other hand exhibits a significantly lower R-value. The deviation from the model behavior might be caused by effects that are not accounted for in the model, like edge effects, uneven pressure or temperature distribution or stretching of the composite fabric. The differences between *UTwente* and *KU Leuven* are slightly more pronounced for the steady state than for the peak CoF's. This might be caused by an inhomogeneous

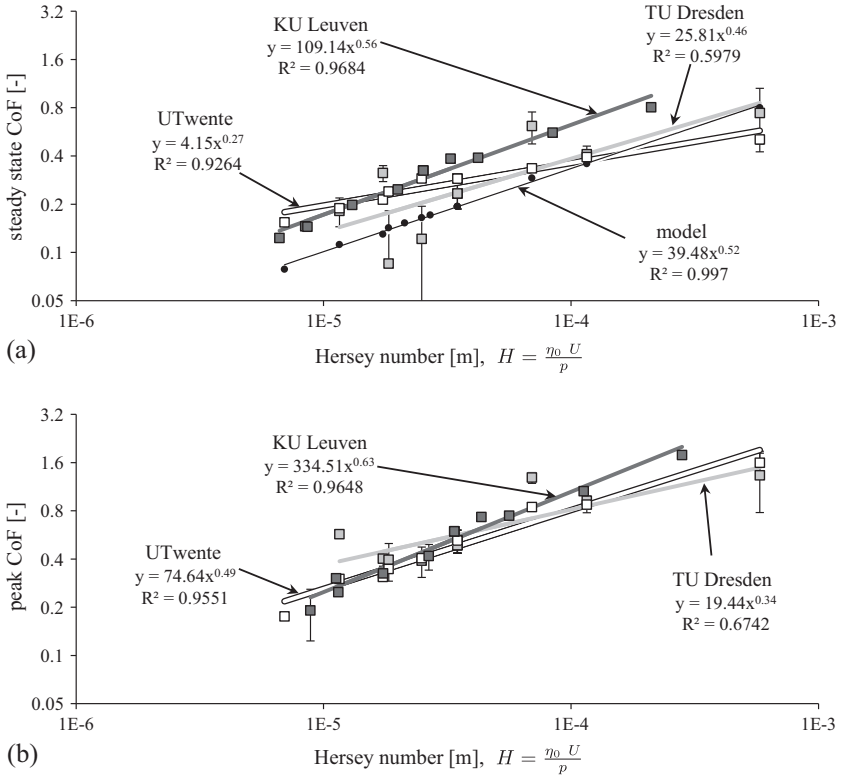

Fig. 11. Stribeck curve, (a) steady state and (b) peak friction.

pressure distribution, that is likely to develop during an experiment with a pull-out configuration. Ten Thije and Akkerman [15] have shown by means of numerical models that different pressure distributions with an identical average pressure can influence the apparent hydrodynamic friction coefficient significantly. Therefore, it is important to evaluate the pressure and temperature distributions of the set-up thoroughly. This poses a challenge, especially when they are expected to be influenced by the friction dynamics. Also edge effects can play a role, in particular at the location where virgin material is pulled into the contact area.

6. Conclusions and recommendations

A comparison between different friction test set-ups for thermoplastic composites was made in a friction benchmark exercise. All participants used the same Twintex PP material and started from the same predefined test conditions. Two different types of friction have been tested: dry friction at ambient temperature, which is an Amontons-Coulomb-like friction, and hydrodynamic friction at temperatures above the melting point of the resin. The measurement results of the benchmark participants were fairly consistent. For the dry friction experiments, the resulting CoFs of the participating 7 research groups did not deviate more than 5% from the measured average CoF. However, the results do reveal the presence of systematic errors, since one research group measured consistently higher CoFs than another. This was attributed to edge effects and the size of the friction surface. Uneven pressure distributions due to the set-up design have no significant influence on Amontons-Coulomb friction, but do play a role in the hydrodynamic lubricated friction. The hydrodynamic friction behavior can be described with a master curve known as a Stribeck curve. Measurement data of the considered material obtained by two different research groups are well approximated by such a master curve, where one group uses a pull-out set-up while the other group uses a pull-through set-up. A slightly better agreement between the pull out and the pull through test results is observed for the peak CoF, than for the steady state CoF, which might be related to the development of uneven pressure distributions in pull-out tests.

The current benchmark suggests that friction measurements improve with certain design characteristics of the set-up. Larger friction surfaces reduce the influence of edge effects. Also chamfered edges or pulling the metal foil instead of the composite material can minimize these edge effects. To enhance the start-up response to initial effects, the stretch of fabric has to be limited, e.g. by fixing it rigidly to a surface and using steel foil as the inner specimen that is pulled out. Local heating of the specimen reduces excessive heating times and allows a more immediate measurement of displacement and forces by sensors near the test specimen. Attention should be paid to a uniform pressure and temperature distribution. A pull through design supports uniform pressure distributions, while additional arrangements need to be made to preheat the regions of the specimen material that is initially outside but pulled in between the friction surface.

References

[1] Harrison P, Clifford M. Chapter 3 rheological behaviour of pre-impregnated textile composites. In: Design and manufacture of textile composites. Cambridge, UK: Woodhead Publishing Ltd.; 2005. p. 110148.
[2] Friedrich K, Hou M, Krebs J. Chapter 4 thermoforming of continuous fibre/thermoplastic composite sheets. Composite sheet forming, vol. 11. Elsevier; 1997. p. 91–162.
[3] Haanappel SP. Forming of UD fibre reinforced thermoplastics, doctoral thesis. University of Twente, Enschede; April 2013.
[4] Groves D. A characterization of shear flow in continuous fibre thermoplastic laminates. Composites 1989;20(1):28–32.
[5] Scherer R, Friedrich K. Inter- and intraply-slip flow processes during thermoforming of cf/pp-laminates. Compos Manuf 1991;2(2):92–6.
[6] Morris S, Sun C. An investigation of interply slip behaviour in AS4/PEEK at forming temperatures. Compos Manuf 1994;5(4):217–24.
[7] Murtagh AM, Lennon JJ, Mallon PJ. Surface friction effects related to pressforming of continuous fibre thermoplastic composites. Compos Manuf 1995;6(34):169–75.
[8] Lebrun G, Bureau MN, Denault J. Thermoforming-stamping of continuous glass fiber/polypropylene composites: interlaminar and tool-laminate shear properties. J Thermoplast Compos Mater 2004;17(2):137–65.
[9] Gorczyca-Cole JL, Sherwood JA, Chen J. A friction model for thermostamping commingled glasspolypropylene woven fabrics. Compos Part A: Appl Sci Manuf 2007;38(2):393–406.
[10] Murtagh AM, Mallon PJ. Chapter 5 characterisation of shearing and frictional behaviour during sheet forming. Composite sheet forming, vol. 11. Elsevier; 1997. p. 163–216.
[11] D20 Committee. Test method for static and kinetic coefficients of friction of plastic film and sheeting, Tech. rep., ASTM International; 2001.
[12] Vanclooster K. Forming of multilayered fabric reinforced thermoplastic composites, doctoral thesis. KU Leuven, Leuven; 2010.
[13] Ubbink M. Tool–ply friction of woven fabric composites, Ph.D. thesis. University of Twente, Enschede, the Netherlands; July 2006.
[14] Akkerman R, Ten Thije R, Sachs U, De Rooij M. Friction in textile thermoplastic composites forming. In: Proceedings of the 10th international conference on textile composites – TEXCOMP 10: recent advances in textile composites; 2010. p. 271–79.
[15] ten Thije R, Akkerman R. Design of an experimental setup to measure tool–ply and ply–ply friction in thermoplastic laminates. Int J Mater Forming 2009;2:197–200.
[16] Jannink P. Karakteriseren van materiaalgedrag van vezelversterkte thermoplasten onder smelt, Ph.D. thesis. Saxion University of Applied Science, Enschede, the Netherlands; September 2009.
[17] Hivet G, Allaoui S, Cam B, Ouagne P, Soulat D. Design and potentiality of an apparatus for measuring yarn/yarn and fabric/fabric friction. Exp Mech 2012;52(8):1123–36.
[18] Brinkmann B. Internationales Wörterbuch der Metrologie: Grundlegende und allgemeine Begriffe und zugeordnete Benennungen (VIM) Deutsch-englische Fassung ISO/IEC-Leitfaden 99: 2007. Beuth Verlag; 2012.
[19] ten Thije R, Akkerman R, Ubbink M, van der Meer L. A lubrication approach to friction in thermoplastic composites forming processes. Compos Part A: Appl Sci Manuf 2011;42(8):950–60.
[20] Bird RB, Armstrong RC, Hassager O. Dynamics of polymeric liquids. Fluid mechanics, 2nd ed., vol. 1. New York, NY: John Wiley and Sons Inc.; 1987.